The Journal of Chemical Physics

Phospholipid acyl tail affects lipid headgroup orientation and membrane hydration

Cite as: J. Chem. Phys. **156**, 234706 (2022); https://doi.org/10.1063/5.0092237
Submitted: 22 March 2022 • Accepted: 24 May 2022 • Published Online: 17 June 2022

Daria Maltseva, Grazia Gonella, Jean-Marie Ruysschaert, et al.

The Journal of Chemical Physics ARTICLE scitation.org/journal/jcp

Phospholipid acyl tail affects lipid headgroup orientation and membrane hydration

Cite as: J. Chem. Phys. 156, 234706 (2022); doi: 10.1063/5.0092237
Submitted: 22 March 2022 • Accepted: 24 May 2022 •
Published Online: 17 June 2022

Daria Maltseva,[1] Grazia Gonella,[1,2] Jean-Marie Ruysschaert,[3] and Mischa Bonn[1,a)]

AFFILIATIONS

[1] Max Planck Institute for Polymer Research, Ackermannweg 10, 55128 Mainz, Germany
[2] Institute of Biochemistry, ETH Zurich, Otto-Stern-Weg 3, 8093 Zurich, Switzerland
[3] Laboratory for the Structure and Function of Biological Membranes, Université Libre de Bruxelles, Boulevard du Triomphe, 1050 Brussels, Belgium

[a)] **Author to whom correspondence should be addressed:** bonn@mpip-mainz.mpg.de

ABSTRACT

Biomembrane hydration is crucial for understanding processes at biological interfaces. While the effect of the lipid headgroup has been studied extensively, the effect (if any) of the acyl chain chemical structure on lipid-bound interfacial water has remained elusive. We study model membranes composed of phosphatidylethanolamine (PE) and phosphatidylcholine (PC) lipids, the most abundant lipids in biomembranes. We explore the extent to which the lipid headgroup packing and associated water organization are affected by the lipid acyl tail unsaturation and chain length. To this end, we employ a combination of surface-sensitive techniques, including sum-frequency generation spectroscopy, surface pressure measurements, and Brewster angle microscopy imaging. Our results reveal that the acyl tail structure critically affects the headgroup phosphate orientational distribution and lipid-associated water molecules, for both PE and PC lipid monolayers at the air/water interface. These insights reveal the importance of acyl chain chemistry in determining not only membrane fluidity but also membrane hydration.

INTRODUCTION

Lipids are ubiquitous in nature and fulfill a wide range of functions varying from providing membrane structure to information transduction and energy storage.[1,2] In particular, lipids constitute the main component of the cell membrane and determine its physical properties.[3,4] In eukaryotic cell membranes, major building blocks are glycerophospholipids, and, among these, the most abundant are lipids with zwitterionic phosphatidylethanolamine (PE) and phosphatidylcholine (PC) headgroups.[2] The lipid headgroup chemical structure plays a significant role in determining the membrane properties. The PE lipid headgroup is relatively small and has both intra- and intermolecular hydrogen-bond donating and accepting ability. The PC headgroup is bulkier than that of PE. Additionally, for the PC headgroup, intermolecular hydrogen bonding is not possible.[5] As a result, the intermolecular interaction between PE headgroups is, in general, stronger than that between the PC headgroups leading to reduced hydration of PE.[6–8] Membrane phospholipids do differ not only in the headgroup but also in the length and degree of saturation of the acyl chain.[9,10] Besides the lipid headgroup chemical nature and size, the structure of the acyl chain also strongly affects the membrane properties.[3] Generally speaking, PE lipids resemble cylinders in the case of saturated acyl chains and cones when the acyl chains contain one or more unsaturated bonds. Saturated PEs form a lamellar phase, and unsaturated PEs form an inverted hexagonal H_{II} phase.[7,11–13] For this reason, unsaturated PE is commonly called a non-bilayer or a curvature-inducing lipid.[13] PE lipids are important for transient membrane structures due to their fusogenic properties.[14–16] Lipids with PC headgroups, independently on the degree of saturation of their tails, generally have more cylindrical shape than PE ones and form a lamellar, or a bilayer, phase, which is of paramount importance for cellular compartmentalization.[8,17]

Many biological processes in the cell occur at the membrane–water interface. The membrane composition and the

related physicochemical and structural properties are crucial for peptides/proteins interacting with membranes.[17–20] For a long time, such interactions were studied without taking water into account, and the solvent was treated as a passive bystander, typically as a dielectric continuum. More recently, this view has been revised, and the role of water as a functional component mediating biomolecular interactions at membranes has been recognized.[21–25] In fact, the hydration state of PE and PC is significant for membrane-associated processes and has been widely studied both experimentally and through computer simulations.[6–8,24,26–28] With the development of surface-sensitive techniques such as vibrational sum-frequency generation (SFG) spectroscopy, much attention has been given to selectively probing water at model membrane interfaces. SFG spectroscopy is a second-order nonlinear optical technique allowing one to probe vibrational modes of molecules located at interfaces.[29–31] The SFG response from molecules in isotropic bulk cancels out due to symmetry considerations and can only be generated at the interface where the inversion symmetry is broken. The SFG signal is sensitive to both the number density and ordering of molecules at the interface and is nonzero if there is a net ordering of interfacial molecular species. Along with surface-specific information, SFG also provides chemically specific information. Since the vibrational frequencies of various functional groups and those of different vibrations (e.g., stretch and bend) within the same moiety are different, these can be resolved spectrally.

The effect of the lipid headgroup net charge on the interfacial water molecular organization has been thoroughly investigated by applying SFG spectroscopy.[32–34] As a model biomembrane, the lipid monolayer formed at the air/water interface has been used,[35–37] which is a reasonable approximation, given the weak interaction between the two leaflets of a bilayer membrane.[36,38,39] SFG studies revealed that negatively and positively charged phospholipid monolayers orient hydrogen atoms of interfacial water molecules toward the interface and the bulk, respectively.[33] Water in the proximity of lipids with zwitterionic headgroups such as PE and PC has likewise been extensively studied.[32,40–43] H-up interfacial water orientation was observed in MD simulations of zwitterionic 1,2-dimyristoyl-sn-glycero-3-phosphocholine (DMPC) monolayer[40] and heterodyne-detected SFG (HD-SFG) experiments for 1-palmitoyl-2-oleoyl-glycero-3-phosphocholine (POPC), 1,2-dipalmitoyl-sn-glycero-3-phosphocholine (DPPC), and 1,2-dipalmitoyl-sn-glycero-3-phosphoethanolamine (DPPE) lipids.[32,43,44] By comparing biologically relevant PC (1,2-dioleoyl -sn-glycero-3-phosphocholine) with synthetic CPe (2-((2,3-bis(oleoyloxy)propyl)-dimethyl-ammonio)ethyl ethyl phosphate) having a reversed headgroup dipole, it was shown that water molecules are mainly oriented by the dipolar field arising from the two oppositely charged molecular moieties within the lipid headgroups.[45] While the effect of different phospholipid headgroups on the organization of lipid-associated interfacial water molecules has been widely investigated, the influence (if any) of the lipid acyl tail on interfacial water has not been reported, to the best of our knowledge. In this study, we focus on zwitterionic PE and PC phospholipid monolayers as model systems for biomembranes. We aim to understand whether the lipid acyl chain parameters (chain length and degree of unsaturation) affect the interfacial water by performing surface-sensitive experiments (SFG spectroscopy, surface pressure measurements, and Brewster angle microscopy).

MATERIALS AND METHODS

Sample preparation

The following six lipids (see structural formulas in Fig. 1) were purchased from Avanti and used as received: 1,2-dipalmitoyl-sn-glycero-3-phosphoethanolamine (16:0 PE, DPPE), 1,2-distearoyl-sn-glycero-3-phosphoethanolamine (18:0 PE, DSPE),

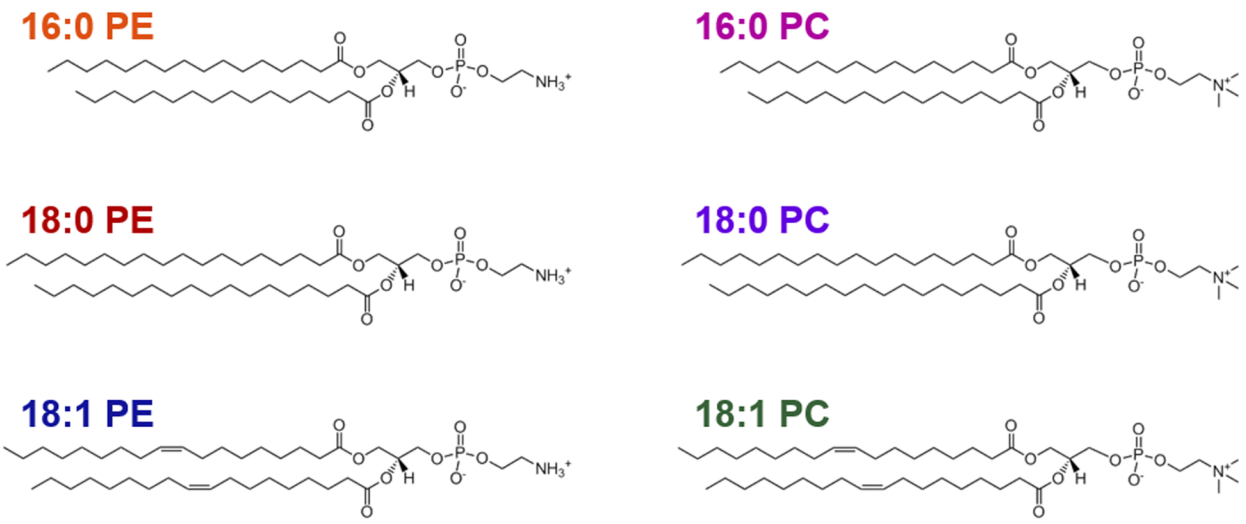

FIG. 1. Structural formulas of PE and PC lipid molecules under investigation.

1,2-dioleoyl-sn-glycero-3-phosphoethanolamine (18:1 PE, DOPE), 1,2-dipalmitoyl-sn-glycero-3-phosphocholine (16:0 PC, DPPC), 1,2-distearoyl-sn-glycero-3-phosphocholine (18:0 PC, DSPC), and 1,2-dioleoyl-sn-glycero-3-phosphocholine (18:1 PC, DOPC). For each phospholipid molecule, a short nomenclature "M:N PX" is used, meaning that each lipid acyl chain contains M carbon atoms and N unsaturated (double) bonds, and "PX" denotes the particular phospholipid headgroup (e.g., PE or PC). For 16:0 PE, 18:1 PE, 16:0 PC, 18:0 PC, and 18:1 PC, lipid stock solutions were prepared by dissolving the lipids in the chloroform/methanol = 9:1 (vol/vol) mixture to the 0.429 mM concentration. Due to lower solubility, the 18:0 PE lipid was dissolved in the chloroform/methanol = 8:2 (vol/vol) mixture to the 0.143 mM concentration. Chloroform was purchased from Fisher Scientific (≥99.8% ACS purity), and methanol was purchased from VMR chemicals (≥99.9% purity).

Surface pressure (SP) measurements were performed with a DeltaPi tensiometer (KBN 315 Sensor Head, Kibron, Inc.) and FilmWareX 3.62 software.

Langmuir pressure–area isotherms were collected in a Langmuir trough (dimensions 220 × 59 mm^2) made of pure Teflon. A barrier with automated motion was made of a hydrophilic material, Delrin. For the isotherm collection, the speed of the barrier movement was set at 5 mm/min. The surface pressure was monitored by the same tensiometer and software mentioned above.

Vibrational sum-frequency generation (SFG) spectroscopy

Detailed descriptions of the homo- and heterodyne-detected SFG spectroscopy setups are provided in the supplementary material (Sec. I). All homodyne SFG spectroscopy experiments reported in the current paper were performed at 22.5 ± 1.0 °C. 20 ml of pure water (H_2O, obtained from ultrapure Millipore Milli-Q machine, resistivity 18.2 MΩ·cm) was added into a thoroughly cleaned polytetrafluoroethylene (PTFE) coated aluminum trough, SP was calibrated at the air/water interface, and the trough was rotated (19–20 rotations per minute). Rotation of the trough was used for averaging over different spots on the sample surface as well as to avoid the steady-state perturbation of a single spot by the laser beam.[46] Afterward, the lipid solution was spread at the air/water interface dropwise with the Hamilton click-syringe (0.5 μl droplet volume). This way of a lipid monolayer preparation was compared with Langmuir monolayer compression, and it provides very similar results; see the supplementary material (Sec. II). The monolayer was left for relaxation (~15 min), and after that, an SFG spectrum was recorded. SP was monitored during the entire experiment. The sample box was flushed with nitrogen to prevent the oxidation of unsaturated lipids.[47,48] To process each homodyne SFG spectrum, the background-corrected sample spectrum was divided by the background-corrected reference spectrum to correct for the spectral shape of the IR beam. The background was recorded by blocking the IR beam. The acquisition time for a background collection was the same as that for a sample spectrum collection. To record the reference, in the CH/OH-stretch spectral region (2800–3600 cm^{-1}), a *z*-cut quartz crystal was used, whereas in the phosphate stretch region (1000–1200 cm^{-1}), a gallium arsenide (GaAs) wafer was used.

Brewster angle microscopy (BAM)[49]

BAM imaging of monolayers at the air/water interface was performed on Accurion (Nanofilm EP3, Accurion) with 10× objective and EP3 View software. The objective focus, polarization optic angles, the sample stage height, the laser power, and the beam incidence angle were adjusted to obtain the optimal image contrast and signal-to-noise ratio. BAM image dimensions are 387 × 500 μm^2.

RESULTS AND DISCUSSION

The effect of the lipid acyl tail on the lipid phosphate group orientation

The phosphate moiety is an important site in the lipid headgroup due to its ability to bind biomolecules and water.[50–52] For zwitterionic lipids, the phosphate–nitrogen (P–N) headgroup dipole mainly determines the interfacial water orientation.[45] The phosphate moiety vibrations are known to be sensitive to the local water environment and report on the membrane hydration state.[53] In order to understand whether the phosphate orientation is affected by slight variations in a chemical structure of the lipid acyl chain (saturation/unsaturation and length), we probe the phosphate moiety stretch vibration, namely, the symmetric PO_2^- stretch centered at ~1100 cm^{-1}; see the schematic representation in Fig. 2(a).[54–56] We note that in the spectral region 1050–1150 cm^{-1}, several contributions are possible besides that from the symmetric PO_2^- stretch mode: headgroup skeletal R–O–P–O–R′ and/or C–O–P stretch at ~1050–1080 cm^{-1}[51,55–58] and (C=O)–O–C antisymmetric stretch at ~1115 cm^{-1}.[58,59]

Figures 2(b) and 2(c) show SFG spectra for PE and PC lipid monolayers at the same packing density of 74 $Å^2$/molecule. PE lipid signals are overall roughly two times stronger than for PC. More interestingly, the observed SFG signal for the 16:0 lipid is substantially higher than for 18:1, for both PE and PC headgroups. This is remarkable since the higher SP for the 18:1 lipids [see insets of Figs. 2(b) and 2(c)] would suggest enhanced lipid order[54,60] and, thus, would result in higher SFG signal. Since the number of molecules is the same, the difference in the SFG signal intensity must originate from the different orientations of the transition dipole moments (TDMs). For the PO_2^- symmetric stretch vibrational mode, the TDM is antiparallel to the bisector of the OPO^- angle as presented in Fig. 2(d). The low SFG signal for 18:1 could be due to (1) a more randomized orientational distribution of the PO_2^- TDM, (2) an, on average, more parallel to the interfacial plane TDM in comparison to that of 16:0, and (3) a combination of the two. However, what could be the origin of the different TDM orientational distribution?

As can be seen in the Langmuir surface pressure–area isotherms describing the monolayer phase state at a fixed temperature and presented in the inset of Figs. 2(b) and 2(c), the 16:0 and 18:1 lipids at 74 $Å^2$/molecule are in different monolayer phase states. Namely, 16:0 PE is in gas (G) phase characterized by surface pressure $\pi \sim 0$ mN/m, while 18:1 PE is in the liquid expanded (LE) phase. Similarly, 16:0 PC is in an intermediate phase, which is a mixture of LE and liquid condensed (LC) domains, while 18:1 PC is in the LE phase. BAM images were obtained for PE and PC monolayers at various packing densities and, thus, various monolayer phase states at a fixed temperature and are presented in the supplementary material

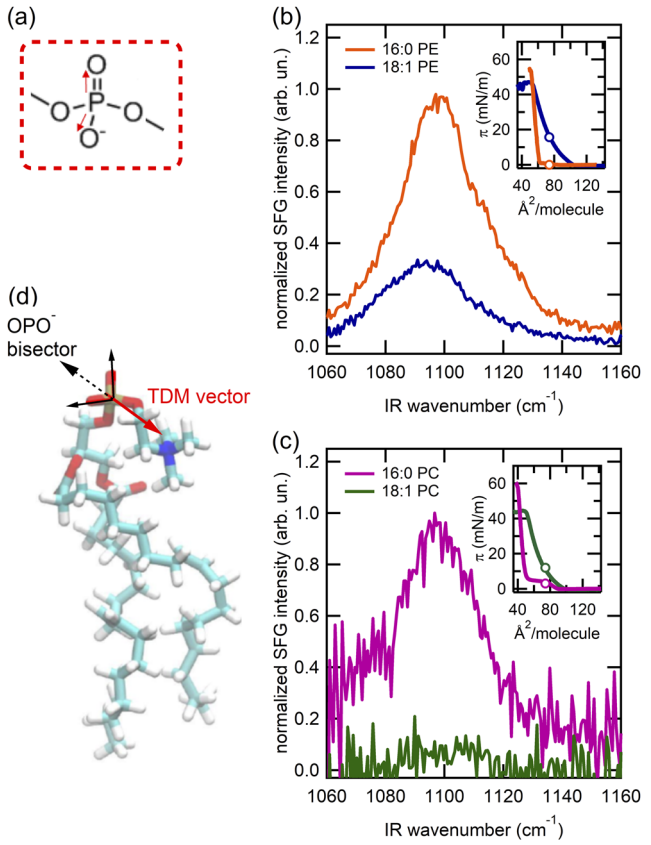

FIG. 2. Normalized SFG spectra acquired in the ssp polarization combination in the phosphate stretch region with the peak centered at 1100 cm^{-1} corresponding to the (a) symmetric PO_2^- stretch vibration for (b) (orange) 16:0 PE and (blue) 18:1 PE and (c) (pink) 16:0 PC and (green) 18:1 PC lipid monolayers at 74 Å^2/molecule. In the inset graphs, Langmuir surface pressure–area isotherms for each lipid are presented. The open circles indicate 74 Å^2/molecule. (d) The OPO^- bisector and the antiparallel transition dipole moment (TDM) of the symmetric PO_2^- stretch vibration.

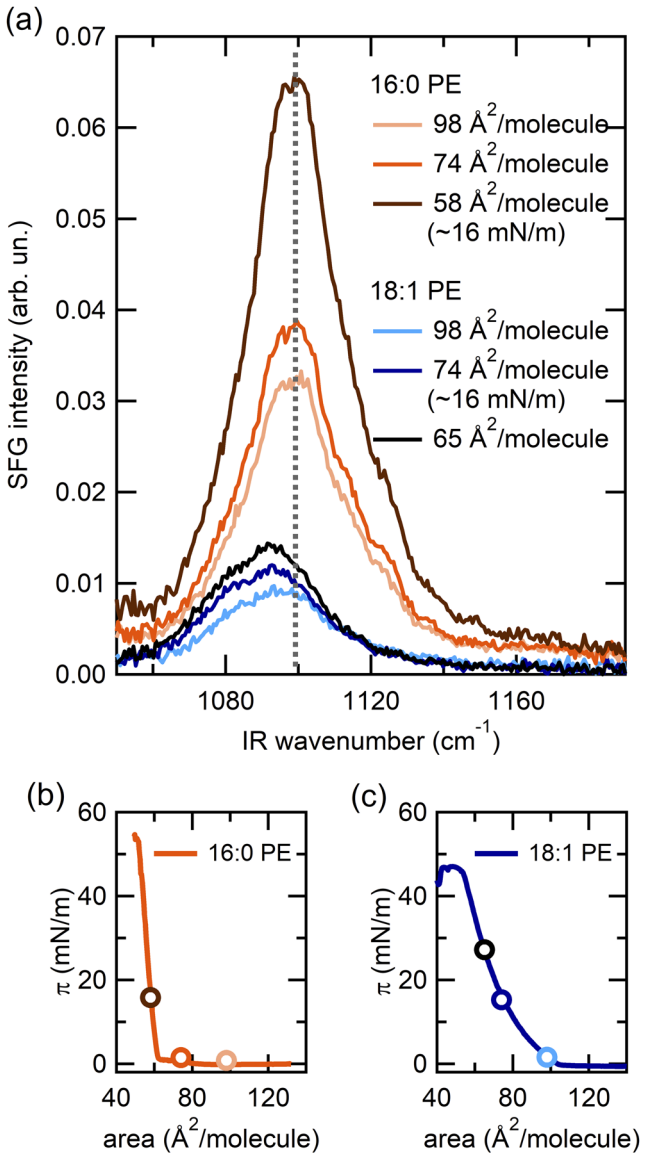

FIG. 3. (a) SFG spectra acquired in ssp polarization combination in the phosphate stretch region with the peak centered at 1100 cm^{-1} corresponding to the symmetric PO_2^- stretch vibration for (orange curves) 16:0 PE and (blue curves) 18:1 PE monolayers at various packing densities indicated with open circles for (b) 16:0 PE and (c) 18:1 PE lipid monolayers. The dashed line in (a) is to guide the eye to the center frequency of the spectra for 16:0 PE.

(Sec. III). The PE and PC monolayers exhibit different morphologies (levels of heterogeneity) in different phase states, which would be consistent with the different SFG signals obtained for 16:0 and 18:1 lipids. To investigate whether the differences in SFG intensity observed in Figs. 2(b) and 2(c) are due to the difference in a lipid monolayer phase state (i.e., G, LE, or LE-LC), we performed SFG experiments for both 16:0 and 18:1 PE monolayers at various packing densities. Figure 3 shows the corresponding SFG spectra. The data clearly show that, independently of the lipid packing density, the SFG signal from PO_2^- stretch is higher for the 16:0 PE monolayer than for 18:1 PE, thus ruling out the different lipid packing density and associated surface pressure from the possible reasons of the observed SFG signal difference.

We note that the lipid state is not only determined by the packing density, as shown in the insets of Figs. 2(b) and 2(c), but also a function of temperature. In fact, the gel–liquid–crystalline (melting) phase transition temperatures for PE (PC) bilayers composed of saturated vs unsaturated lipids are dramatically different: For 16:0 and 18:1, they are 64 (42) and −7 (−18 °C), respectively.[61] Given that our experiments are conducted at room temperature (22.5 ± 1.0 °C), the origin of the different molecular organization of 16:0 vs 18:1 is likely the following: independent of surface pressure, the orientational distribution is likely broader for 18:1 lipid, which is in the more disordered crystalline phase compared to 16:0, which is in the more ordered gel phase.

In fact, the unsaturated bond leads to a low ordering of acyl chains, as was reported previously.[62,63] We suggest that disordered acyl chains affect the lipid headgroup organization, which, in turn, leads to the orientational disorder of moieties within the headgroup. We propose that for 18:1, the lipid disorder is, indeed, the major cause of the low SFG signal intensity, rather than the possible in-plane orientation of the PO_2^- TDM. However, the latter effect cannot be completely excluded. In connection with this, we propose that the width of the orientational distribution of the PO_2^- moiety is broad for 18:1 compared to more narrow for 16:0. This suggests that small variations in the chemical structure of the acyl tail (16:0 vs 18:1) substantially affect the orientational ordering of the headgroup PO_2^- moiety.

It is notable that the spectral response of 16:0 PE differs from that of 18:1 PE not only by intensity but also by the position of the center peak frequency [see Fig. 3(a) and Table S1 for fitting results]. An interesting observation is that at all lipid packing densities considered, the 18:1 PE spectrum was found to be red-shifted by ~9 cm^{-1} with respect to that of 16:0 PE. Taking into account the previously established sensitivity of the PO_2^- stretch toward the local water structure,[53] the difference we have detected indicates a distinct lipid hydration environment of 18:1 vs 16:0 PE. We attribute the red-shift of the phosphate band to PO_2^- moieties more strongly hydrogen-bonded to water molecules in the case of 18:1. The proposed difference in hydration possibly results from a different lipid headgroup packing, ordered for 16:0 PE vs disordered for 18:1 PE, leading to a different water molecular distribution. In fact, considering the ability of the phosphate group to form a hydrogen bond with the amine group of a neighboring PE lipid molecule,[5] the more ordered headgroup organization of 16:0 can likely facilitate the intermolecular hydrogen bond formation, which would lead to headgroup dehydration. Analogously, in a previous study, a similar difference in the center frequency of the symmetric PO_2^- stretch vibrational response was reported for the DPPC lipid monolayer in loosely packed LE vs the ordered LC phase state, assigned to the difference in the lipid hydration state, namely, to more strongly hydrated lipid headgroups in LE compared to less hydrated in the LC state.[54]

In summary, we revealed a prominent effect of the lipid acyl tail chemical structure on phosphate orientation (ordered for 16:0 and more randomized for 18:1) and, tentatively, on lipid hydration. Motivated by the fact that the phosphate group forms strong hydrogen bonds with water molecules and that these bonds are directional, we investigate if there is any effect of the chemical structure of lipid acyl tail on lipid-bound water organization by directly probing water vibrations.

The effect of the lipid acyl tail on interfacial water

We explore interfacial water by probing OH-stretch vibrations of hydrogen-bonded water molecules at the lipid interface. Figures 4(a) and 4(b) display SFG spectra for 16:0, 18:0, 18:1 PE and PC lipid monolayers at 74 $Å^2$/molecule in the CH-/OH-stretch region. Langmuir pressure–area isotherms indicating the lipid state of each monolayer at 74 $Å^2$/molecule are presented in Figs. 5(a) and 5(b).

In Fig. 4, the SFG signal in the spectral range of 2800–3000 cm^{-1} is generated by various CH-stretch vibrational

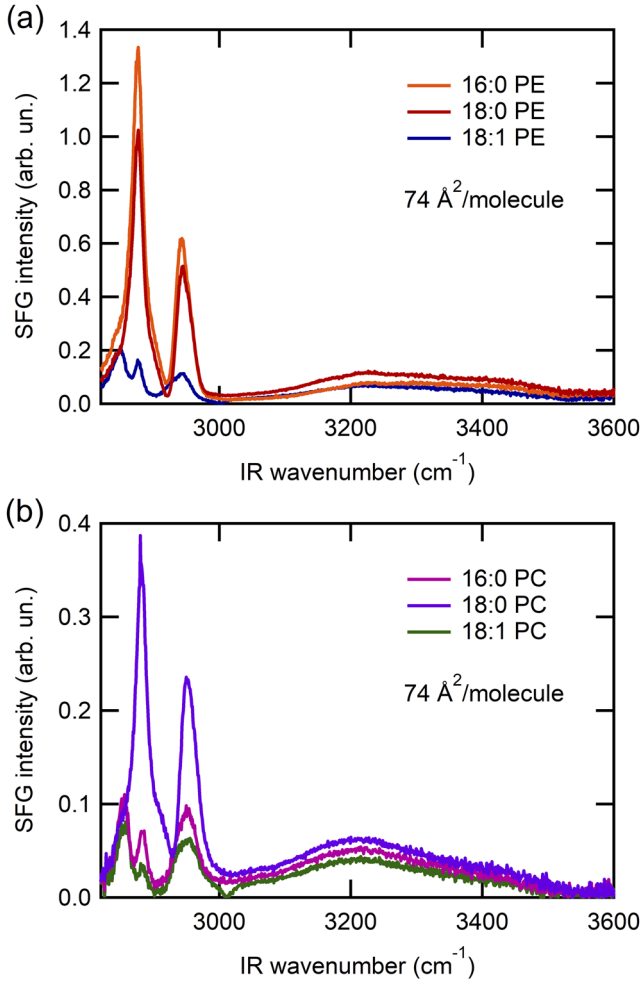

FIG. 4. SFG spectra in the CH- and OH-stretch region for (a) PE and (b) PC lipid monolayers at 74 $Å^2$/molecule.

modes: CH_2 symmetric centered at ~2850 cm^{-1}, CH_3 symmetric at ~2880 cm^{-1}, CH_3 Fermi resonance at ~2940 cm^{-1}, CH_3 asymmetric at ~2960 cm^{-1}, and vinyl CH at ~3010 cm^{-1} (present only for unsaturated lipids).[31] The spectra for 16:0 PE, 16:0 PC, and 18:1 PC are in good agreement with the reported ones measured at similar packing densities.[45,60,64,65]

CH vibrations provide information on the ordering in a monolayer. For the lipid monolayer composed of lipids with saturated acyl chains, CH_3 (symm)/CH_2 (symm) signal ratio is an order parameter.[31,66] For a highly ordered lipid monolayer, acyl chains are in all-trans conformation and the ratio value is high, since the CH_3 symmetric stretch signal is high due to CH_3 moieties located in terminal methyl groups exhibiting high ordering. On the contrary, the CH_2 symmetric stretch signal is small because CH_2 moieties are located in a locally centrosymmetric environment leading to SFG signal cancellation. In contrast, for disordered acyl chains, the ratio value is low: the CH_2 symmetric stretch signal is high because

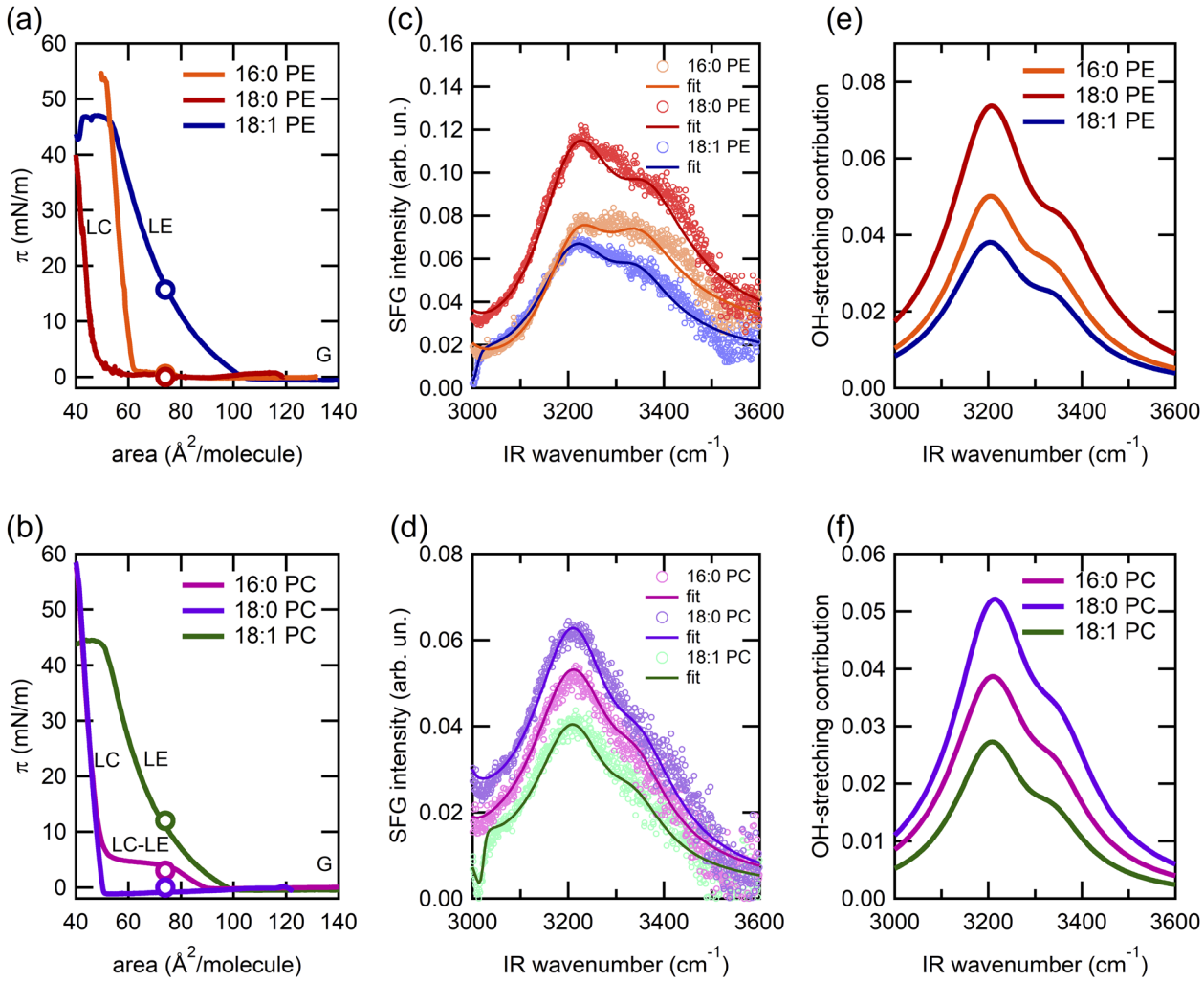

FIG. 5. Langmuir pressure–area isotherms (solid lines) for (a) PE and (b) PC monolayers. For each monolayer, an open circle represents the point on the curve corresponding to 74 Å^2/molecule. SFG spectra zoomed-in the OH-stretch region for (c) PE and (d) PC lipid monolayers (open circles) and the corresponding fit curves (solid lines). The OH-stretch contributions for (e) PE and (f) PC monolayers were obtained from the SFG spectral fitting.

gauche defects in disordered acyl chains break the local centrosymmetry of the CH_2 environment, whereas the CH_3 symmetric stretch response is naturally low because terminal groups of disordered acyl chains are also disordered. It is worth to note that the CH_3 (symm)/CH_2 (symm) order parameter cannot be applied in the case of unsaturated chains, due to the C=C bond by itself already breaking the symmetry by creating a kink in the lipid structure. In this case, the CH_3 symmetric stretch signal serves as an order parameter. This allows us to compare acyl chain ordering in 16:0, 18:0, and 18:1 monolayers. For PE, based on CH_3 symmetric stretch peak amplitudes obtained from fitting (Table S2 in the supplementary material), we conclude that 16:0 PE and 18:0 PE monolayers are significantly more ordered than 18:1 PE and that 18:0 PE is slightly more ordered than 16:0 PE (Tables S4 and S5). Among the considered PC lipids (Table S3 in the supplementary material), 18:0 PC is substantially more ordered compared to 16:0 PC and 18:1 PC, and 16:0 PC is more ordered than 18:1 PC (Table S6). Interestingly, for the saturated 16:0 PC, more pronounced acyl chain ordering would be expected; however, at the same time, the 16:0 PC SFG spectrum is consistent with the published ones measured at a similar packing density of 74 Å^2/lipid.[60,65] We hypothesize that this could be explained by (1) the local increase of the temperature at the focus point of beams at the surface despite the trough rotation, taking into account that the gel–liquid crystalline phase transition temperature T_m for 16:0 PC is equal to ~42 °C (Table S6) and is the closest to the temperature of the experiment (~22.5 °C) compared to T_m values of other considered lipids, and/or (2) the fact that 74 Å^2/lipid for 16:0 PC lipid monolayer is close to the inflection point between the LE and LE-LC coexistence phases at the surface pressure–area isotherm [Fig. 5(b)] and therefore might not be stable thermodynamically.

The spectral range of 3000–3600 cm^{-1} corresponds to the OH-stretch vibration of hydrogen-bonded water molecules. The CH- and OH-stretch responses partly overlap in frequency, and for some of the saturated lipids, the CH signal is quite intense. Hence, there is, in general, a spectral interference between the two responses. To extract the OH-stretch contribution, the SFG spectra are fitted to the following function:

$$\chi^{(2)}(\omega) = A_{NR}e^{i\phi_{NR}} + \sum_j \frac{A_j}{\omega - \omega_{IR,j} + i\Gamma_j}, \quad (1)$$

where A_{NR} and ϕ_{NR} are the amplitude and phase of the non-resonant contribution. Each vibrational resonance is represented by a Lorentzian line shape with amplitude A, center frequency ω_{IR}, and half-width at a half maximum (HWHM) Γ.[31] The signs for CH and OH signals were chosen according to the zwitterionic POPC lipid spectrum obtained in heterodyne-detected SFG (HD-SFG) studies reported by Mondal *et al.*[43]

Figures 5(c) and 5(d) show the zoomed-in OH-stretch spectral region for PE and PC, respectively (open circles). Solid lines are the fitting curves. Fit parameters are presented in the supplementary material in Table S2 for PE and Table S3 for PC lipid monolayers. Figures 5(e) and 5(f) display the spectra of the OH-stretch vibration obtained from the fit in the case of PE and PC lipids, respectively. We note that the inferred water responses are in good agreement with phase-resolved measurements shown in Fig. 6. For both PE and PC, the interfacial water response is such that $I_{OH}(18:0) > I_{OH}(16:0) > I_{OH}(18:1)$. This evidence suggests that the interfacial water is affected by both the lipid acyl tail length and its saturation. We propose that the disorder in acyl chains packing introduced by the double bond (18:1 vs 18:0) and a slightly shorter acyl chain (16:0 vs 18:0) leads to more disordered packing of lipid headgroups, which influences the orientational distribution of the phosphate moiety, which, in turn, affects interfacial water ordering. We note that one may expect differences between the different O–H stretch responses, given the different strength of the hydrogen bonds around the head groups. The O–H stretch response is governed by several other H-bonding interactions of water,[41,43] which apparently obfuscate the effects due to variation in phosphate binding.

To compare the interfacial water associated with PE and PC headgroups, we further probe the OH-stretch vibration of the hydrogen-bonded water molecules. To improve the signal-to-noise ratio, we employ heterodyne-detected SFG (HD-SFG) spectroscopy. Another advantage of HD-SFG spectroscopy is that, in comparison with homodyne SFG detection, the obtained spectrum of the imaginary part of the second-order nonlinear susceptibility, $\mathrm{Im}(\chi^{(2)})$, is free from non-resonant contribution. We performed HD-SFG experiments on 18:0 PE and 18:0 PC lipid monolayers at ~20 mN/m, i.e., close to biomembrane conditions. 18:0 lipids were selected, since the SFG signal intensity for 18:0 is the highest among the considered acyl chains (Fig. 5). $\mathrm{Im}(\chi^{(2)})$ spectra for these lipid monolayers are presented in Fig. 6, and the reconstructed homodyne SFG spectra are shown in Fig. S11(a). Also here, the signals in the 2800–3000 cm^{-1} region originate from lipid CH-vibrations, and the response in 3000–3600 cm^{-1} region originates from OH-stretch vibrations of the water molecules associated with lipids within their headgroup dipoles. For both PE and PC, $\mathrm{Im}(\chi^{(2)})$

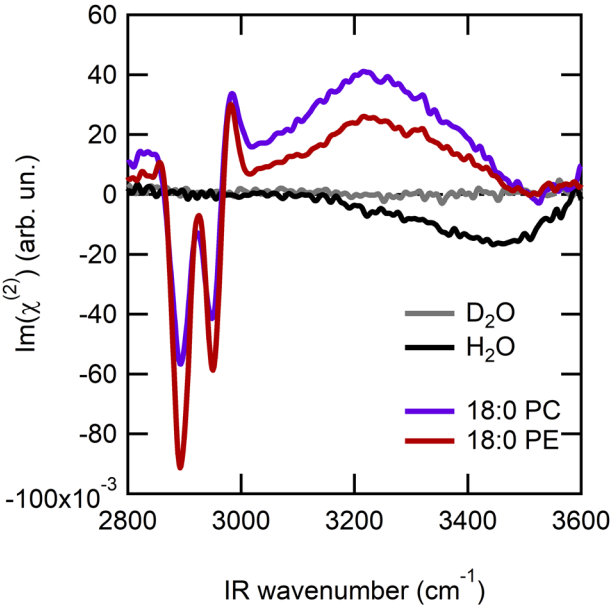

FIG. 6. The imaginary part of the second-order susceptibility obtained from HD-SFG measurements: (gray) D_2O, (black) H_2O, (purple) 18:0 PC lipid monolayer, and (red) 18:0 PE lipid monolayer. Lipid monolayers were measured at ~20 mN/m.

of the OH signal has a positive sign, evidence of the net H-up orientation of interfacial water molecules, in agreement with previous studies of zwitterionic lipid monolayers.[32,43] D_2O and H_2O spectra are presented as standard samples. Figure 6 shows that the OH-signal intensity is higher for PC compared to that for the PE lipid monolayer, while their spectral shapes are indistinguishable. As theoretically predicted by Roy *et al.* for POPE (1-palmitoyl-2-oleoyl-sn-glycero-3-phosphoethanolamine) and POPC, a smaller signal for PE is observed, which is assigned to the lipid headgroup–water hydrogen bonds: for PE that leads to more downward orientation—hydrogen atoms pointing down—of water molecules around the amine group.[28] In contrast, water around choline is oriented more randomly like a clathrate around the nonpolar moiety. It suggests that a more pronounced disorder around the choline group leads to an imperfect cancellation of the signal produced by the hydrogen-bonded water around the phosphate headgroup, which results in a slightly higher positive signal for PC. The higher intensity for 18:0 PC in comparison with 18:0 PE is also in good agreement with experimental data reported for 16:0 PC and 16:0 PE [and our data in Fig. S11(b)],[32] indicating that the difference in the lipid PE vs PC headgroup-bound water organization does not depend on the chemical structure of acyl tails.

Summarizing our studies on PE and PC, the most abundant zwitterionic lipids in eukaryotic (sub)cellular membranes, we aimed at revealing whether the membrane-associated water organization is affected by small variations in the chemical structure of lipid acyl chains. For both PE and PC, we observe the prominent effect of the lipid acyl chain unsaturation and/or length on

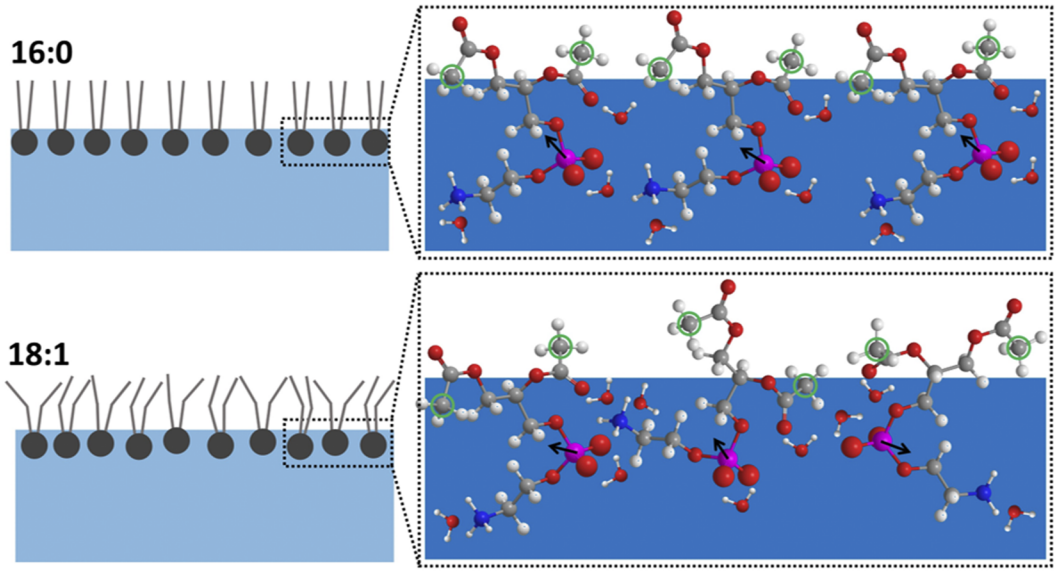

FIG. 7. Proposed model of the lipid and lipid-bound interfacial water organization for 16:0 vs 18:1 lipid monolayers for (top) 16:0 PE and (bottom) 18:1 PE. A similar model applies to 16:0 PC and 18:1 PC. In the sketches on the right side (pictures created in Chem3D), the white, gray, blue, red, and purple balls indicate hydrogen, carbon, nitrogen, oxygen, and phosphorus atoms, respectively. Green circles indicate carbon atoms where the acyl chain connects. Black arrows represent the transition dipole moment vectors of the OPO^- headgroup moiety, which are substantially more ordered in the case of a 16:0 than an 18:1 monolayer. Such a phosphate orientational distribution affects the interfacial water organization, resulting in more ordered water molecules for a 16:0 than an 18:1 monolayer.

the ordering of the PO_2^- moiety of the lipid headgroup, by comparing 16:0 with 18:1 lipids. This lipid tail-dependent effect most likely arises from the difference in the width of the orientational distribution of the phosphate moiety. The gel–crystalline phase transition temperatures of the 18:1 and 16:0 lipids are far below and far above room temperature, respectively, resulting in the higher disorder for the 18:1 acyl chains. We propose that the observed effect likely is primarily due to the acyl chain unsaturation significantly decreasing the acyl chain order, which, in turn, affects the lipid packing. The lipid packing (ordered vs disordered) in turn affects lipid headgroup ordering, i.e., the headgroup orientational distribution. We show that the interfacial water response is also sensitive to the acyl tail. We hypothesize that the chemical structure of the phospholipid tail affects the interfacial water ordering through the orientational distribution of the phosphate moiety. Namely, a more randomized phosphate moiety orientation results in a more randomized orientation of lipid-bound water molecules and vice versa.

To summarize our results pictorially, we draw a schematic model of the lipid and lipid-bound interfacial water organization (Fig. 7) consistent with our results. On the left side of Fig. 7, we present a schematic picture of the acyl chain ordering, prominent for 16:0 and low for 18:1 lipid monolayers, consistent with previous studies of saturated vs unsaturated lipids and in agreement with our results. On the right side of Fig. 7, for simplicity, we do not draw lipid acyl chains but rather zoom in the interfacial region where lipid headgroups and headgroup-associated water molecules interact. In this picture model created for 16:0 and 18:1 PE lipid monolayers using the Chem3D program, we highlight that headgroups of 16:0 lipids are more ordered in comparison with those of 18:1. For each lipid molecule, the black arrow indicates the orientation of the transition dipole moment of the PO_2^- moiety. Naturally, these dipole moments are more randomized in the case of 18:1 as a result of headgroup orientational disorder. In contrast, for 16:0, these dipole moments present a clear net orientation. For both monolayers, water molecules in the vicinity of headgroup moieties are depicted. We emphasize that the amount of net oriented water is higher for the 16:0 lipid monolayer which possesses the higher headgroup ordering. A similar molecular picture is proposed for 16:0 and 18:1 PC lipid monolayers.

CONCLUSIONS

For both PE and PC, for lipids that differ only by the acyl chain unsaturation and length, we observe a distinct lipid headgroup organization and associated water ordering. This highlights the importance of the alkyl chain in determining not only membrane fluidity but also membrane hydration. Our work is novel in unveiling the crucial role the acyl tail (and not exclusively the lipid headgroup) chemical structure plays in lipid packing and the interconnected ordering of lipid-associated water and furthers our understanding of biomembrane hydration.

SUPPLEMENTARY MATERIAL

The supplementary material includes the SFG spectroscopy setup description (Sec. I), Langmuir compression vs monolayer

preparation in the SFG trough with the fixed area (Sec. II), Brewster Angle Microscopy (BAM) images of PE and PC monolayers at various packing densities (Sec. III), fitting parameters for the SFG spectra of the 18:1 and 16:0 PE lipid monolayers measured in the phosphate stretch region (Sec. IV), fitting parameters for the SFG spectra of the PE and PC lipid monolayers measured in the CH-/OH-stretch region (Sec. V), CH_2 and CH_3 symmetric stretch contributions for PE and PC monolayers (Sec. VI), and PE vs PC at 20 mN/m: homodyne SFG intensities (Sec. VII).

ACKNOWLEDGMENTS

The authors are very grateful to Takakazu Seki for support with the HD-SFG setup and HD-SFG data processing and to Yuki Nagata, Maksim Grechko, Ellen H. G. Backus, and Konrad Meister for helpful discussions. This work was supported by the MaxWater Initiative from the Max Planck Society.

AUTHOR DECLARATIONS

Conflict of Interest

The authors have no conflicts to disclose.

Author Contributions

Daria Maltseva: Conceptualization (equal); investigation (equal); Methodology (equal); validation (equal); writing – original draft (equal); Writing – review & editing (equal). **Grazia Gonella:** Conceptualization (equal); data curation (equal); methodology (equal); Project administration (equal); supervision (equal); writing – original draft (equal); writing – review & editing (equal). **Jean-Marie Ruysschaert:** Conceptualization (equal); data curation (equal); methodology (equal); supervision (equal); writing – original draft (equal); writing – review & editing (equal). **Mischa Bonn:** Conceptualization (equal); data curation (equal); funding acquisition (equal); methodology (equal); project administration (equal); Resources (equal); supervision (equal); writing – original draft (equal); writing – review & editing (equal)

DATA AVAILABILITY

The data that support the findings of this study are available from the corresponding author upon reasonable request.

REFERENCES

[1]D. Casares, P. V. Escribá, and C. A. Rosselló, "Membrane lipid composition: Effect on membrane and organelle structure, function and compartmentalization and therapeutic avenues," Int. J. Mol. Sci. **20**, 2167 (2019).
[2]G. van Meer, D. R. Voelker, and G. W. Feigenson, "Membrane lipids: Where they are and how they behave," Nat. Rev. Mol. Cell Biol. **9**(2), 112–124 (2008).
[3]A. I. P. M. de Kroon, P. J. Rijken, and C. H. De Smet, "Checks and balances in membrane phospholipid class and acyl chain homeostasis, the yeast perspective," Prog. Lipid Res. **52**(4), 374–394 (2013).
[4]T. Harayama and H. Riezman, "Understanding the diversity of membrane lipid composition," Nat. Rev. Mol. Cell Biol. **19**, 281–296 (2018).
[5]J. M. Boggs, "Lipid intermolecular hydrogen bonding: Influence on structural organization and membrane function," Biochim. Biophys. Acta, Rev. Biomembr. **906**(3), 353–404 (1987).
[6]G. L. Jendrasiak and J. H. Hasty, "The hydration of phospholipids," Biochim. Biophys. Acta, Lipids Lipid Metab. **337**(1), 79–91 (1974).
[7]T. J. McIntosh, "Hydration properties of lamellar and non-lamellar phases of phosphatidylcholine and phospatidylethanolamine," Chem. Phys. Lipids **81**(2), 117–131 (1996).
[8]H. Hauser, I. Pascher, R. H. Pearson, and S. Sundell, "Preferred conformation and molecular packing of phosphatidylethanolamine and phosphatidylcholine," Biochim. Biophys. Acta, Rev. Biomembr. **650**, 21–51 (1981).
[9]B. Antonny, S. Vanni, H. Shindou, and T. Ferreira, "From zero to six double bonds: Phospholipid unsaturation and organelle function," Trends Cell Biol. **25**, 427–436 (2015).
[10]H. I. Ingólfsson, M. N. Melo, F. J. Van Eerden, C. Arnarez, C. A. Lopez, T. A. Wassenaar, X. Periole, A. H. De Vries, D. P. Tieleman, and S. J. Marrink, "Lipid organization of the plasma membrane," J. Am. Chem. Soc. **136**(41), 14554–14559 (2014).
[11]J. N. Israelachvili, *Intermolecular and Surface Forces* (Academic Press, Burlington, MA, 2011).
[12]J. Jouhet, "Importance of the hexagonal lipid phase in biological membrane organization," Front. Plant Sci. **4**, 494 (2013).
[13]J. Li, X. Wang, T. Zhang, C. Wang, Z. Huang, X. Luo, and Y. Deng, "A review on phospholipids and their main applications in drug delivery systems," Asian J. Pharm. Sci. **10**(2), 81–98 (2015).
[14]L. V. Chernomordik and M. M. Kozlov, "Mechanics of membrane fusion," Nat. Struct. Mol. Biol. **15**(7), 675–683 (2008).
[15]G. van Meer and A. I. P. M. de Kroon, "Lipid map of the mammalian cell," J. Cell Sci. **124**(1), 5–8 (2011).
[16]P. R. Cullis, M. J. Hope, and C. P. Tilcock, "Lipid polymorphism and the roles of lipids in membranes," Chem. Phys. Lipids **40**(2–4), 127–144 (1986).
[17]E. Strandberg, D. Tiltak, S. Ehni, P. Wadhwani, and A. S. Ulrich, "Lipid shape is a key factor for membrane interactions of amphipathic helical peptides," Biochim. Biophys. Acta, Biomembr. **1818**(7), 1764–1776 (2012).
[18]O. G. Mouritsen and K. Jørgensen, "A new look at lipid-membrane structure in relation to drug research," Pharm. Res. **15**, 1507–1519 (1998).
[19]E. Jo, J. McLaurin, C. M. Yip, P. St. George-Hyslop, and P. E. Fraser, "α-synuclein membrane interactions and lipid specificity," J. Biol. Chem. **275**(44), 34328–34334 (2000).
[20]J. C. Bozelli and R. M. Epand, "Membrane shape and the regulation of biological processes," J. Mol. Biol. **432**, 5124–5136 (2020).
[21]*Membrane Hydration: The Role of Water in the Structure and Function of Biological Membranes*, 1st ed., edited by E. A. Disalvo (Springer International Publishing, 2015).
[22]J. Fitter, "Interactions of hydration water and biological membranes studied by neutron scattering," J. Phys. Chem. B **103**(38), 8036–8050 (1999).
[23]M. Chaplin, "Do we underestimate the importance of water in cell biology?," Nat. Rev. Mol. Cell Biol. **7**(11), 861–866 (2006).
[24]G. Gonella, E. H. G. Backus, Y. Nagata, D. J. Bonthuis, P. Loche, A. Schlaich, R. R. Netz, A. Kühnle, I. T. McCrum, M. T. M. Koper, M. Wolf, B. Winter, G. Meijer, R. K. Campen, and M. Bonn, "Water at charged interfaces," Nat. Rev. Chem. **5**(7), 466–485 (2021).
[25]M. Chaplin, "Water: Its importance to life," Biochem. Mol. Biol. Educ. **29**(2), 54–59 (2001).
[26]C. Naumann, T. Brumm, A. R. Rennie, J. Penfold, and T. M. Bayerl, "Hydration of DPPC monolayers at the air/water interface and its modulation by the non-ionic surfactant C12E4: A neutron reflection study," Langmuir **11**(10), 3948–3952 (1995).
[27]M. Pasenkiewicz-Gierula, Y. Takaoka, H. Miyagawa, K. Kitamura, and A. Kusumi, "Hydrogen bonding of water to phosphatidylcholine in the membrane as studied by a molecular dynamics simulation: Location, geometry, and lipid–lipid bridging via hydrogen-bonded water," J. Phys. Chem. A **101**(20), 3677–3691 (1997).
[28]S. Roy, S. M. Gruenbaum, and J. L. Skinner, "Theoretical vibrational sum-frequency generation spectroscopy of water near lipid and surfactant monolayer interfaces," J. Chem. Phys. **141**(18), 18C502 (2014).
[29]Y. R. Shen, *Fundamentals of Sum-Frequency Spectroscopy*, Cambridge Molecular Science (Cambridge University Press, 2016).

[30]R. W. Boyd, *Nonlinear Optics*, 3rd ed. (Academic Press, Inc., 2008).
[31]A. G. Lambert, P. B. Davies, and D. J. Neivandt, "Implementing the theory of sum frequency generation vibrational spectroscopy: A tutorial review," Appl. Spectrosc. Rev. **40**(2), 103–145 (2005).
[32]X. Chen, W. Hua, Z. Huang, and H. C. Allen, "Interfacial water structure associated with phospholipid membranes studied by phase-sensitive vibrational sum frequency generation spectroscopy," J. Am. Chem. Soc. **132**(32), 11336–11342 (2010).
[33]J. A. Mondal, S. Nihonyanagi, S. Yamaguchi, and T. Tahara, "Structure and orientation of water at charged lipid monolayer/water interfaces probed by heterodyne-detected vibrational sum frequency generation spectroscopy," J. Am. Chem. Soc. **132**(31), 10656–10657 (2010).
[34]Y. Nojima, Y. Suzuki, and S. Yamaguchi, "Weakly hydrogen-bonded water inside charged lipid monolayer observed with heterodyne-detected vibrational sum frequency generation spectroscopy," J. Phys. Chem. C **121**(4), 2173–2180 (2017).
[35]H. Brockman, "Lipid monolayers: Why use half a membrane to characterize protein-membrane interactions?," Curr. Opin. Struct. Biol. **9**(4), 438–443 (1999).
[36]C. Stefaniu, G. Brezesinski, and H. Möhwald, "Langmuir monolayers as models to study processes at membrane surfaces," Adv. Colloid Interface Sci. **208**, 197–213 (2014).
[37]M. Eeman and M. Deleu, "From biological membranes to biomimetic model membranes," Biotechnol., Agron. Soc. Environ. **14**(4), 719–736 (2010).
[38]M. D. Phan and K. Shin, "Langmuir monolayer: Ideal model membrane to study cell," J. Chem. Biol. Interfaces **2**, 1–5 (2014).
[39]S. Youssefian, N. Rahbar, C. R. Lambert, and S. Van Dessel, "Variation of thermal conductivity of DPPC lipid bilayer membranes around the phase transition temperature," J. R. Soc. Interface **14**(130), 20170127 (2017).
[40]Y. Nagata and S. Mukamel, "Vibrational sum-frequency generation spectroscopy at the water/lipid interface: Molecular dynamics simulation study," J. Am. Chem. Soc. **132**(18), 6434–6442 (2010).
[41]S. Re, W. Nishima, T. Tahara, and Y. Sugita, "Mosaic of water orientation structures at a neutral zwitterionic lipid/water interface revealed by molecular dynamics simulations," J. Phys. Chem. Lett. **5**(24), 4343–4348 (2014).
[42]T. Ohto, E. H. G. Backus, C.-S. Hsieh, M. Sulpizi, M. Bonn, and Y. Nagata, "Lipid carbonyl groups terminate the hydrogen bond network of membrane-bound water," J. Phys. Chem. Lett. **6**(22), 4499–4503 (2015).
[43]J. A. Mondal, S. Nihonyanagi, S. Yamaguchi, and T. Tahara, "Three distinct water structures at a zwitterionic lipid/water interface revealed by heterodyne-detected vibrational sum frequency generation," J. Am. Chem. Soc. **134**(18), 7842–7850 (2012).
[44]W. Hua, D. Verreault, and H. C. Allen, "Solvation of calcium–phosphate headgroup complexes at the DPPC/aqueous interface," ChemPhysChem **16**(18), 3910–3915 (2015).
[45]L. B. Dreier, A. Wolde-Kidan, D. J. Bonthuis, R. R. Netz, E. H. G. Backus, and M. Bonn, "Unraveling the origin of the apparent charge of zwitterionic lipid layers," J. Phys. Chem. Lett. **10**(20), 6355–6359 (2019).
[46]E. H. G. Backus, D. Bonn, S. Cantin, S. Roke, and M. Bonn, "Laser-heating-induced displacement of surfactants on the water surface," J. Phys. Chem. B **116**(9), 2703–2712 (2012).
[47]J. F. D. Liljeblad, V. Bulone, E. Tyrode, M. W. Rutland, and C. M. Johnson, "Phospholipid monolayers probed by vibrational sum frequency spectroscopy: Instability of unsaturated phospholipids," Biophys. J. **98**(10), L50–L52 (2010).
[48]K.-i. Inoue, C. Takada, L. Wang, A. Morita, and S. Ye, "*In situ* monitoring of the unsaturated phospholipid monolayer oxidation in ambient air by HD-SFG spectroscopy," J. Phys. Chem. B **124**(25), 5246–5250 (2020).
[49]D. Hönig and D. Möbius, "Reflectometry at the Brewster angle and Brewster angle microscopy at the air-water interface," Thin Solid Films **210–211**, 64–68 (1992).
[50]M. A. Swairjo, N. O. Concha, M. A. Kaetzel, J. R. Dedman, and B. A. Seaton, "Ca^{2+}-bridging mechanism and phospholipid head group recognition in the membrane-binding protein annexin V," Nat. Struct. Biol. **2**(11), 968–974 (1995).
[51]N. N. Casillas-Ituarte, X. Chen, H. Castada, and H. C. Allen, "Na^+ and Ca^{2+} effect on the hydration and orientation of the phosphate group of DPPC at air–water and air–hydrated silica interfaces," J. Phys. Chem. B **114**(29), 9485–9495 (2010).
[52]A. Melcrová, S. Pokorna, S. Pullanchery, M. Kohagen, P. Jurkiewicz, M. Hof, P. Jungwirth, P. S. Cremer, and L. Cwiklik, "The complex nature of calcium cation interactions with phospholipid bilayers," Sci. Rep. **6**(1), 38035 (2016).
[53]W. Hübner and A. Blume, "Interactions at the lipid–water interface," Chem. Phys. Lipids **96**(1), 99–123 (1998).
[54]G. Ma and H. C. Allen, "DPPC Langmuir monolayer at the air–water interface: Probing the tail and head groups by vibrational sum frequency generation spectroscopy," Langmuir **22**(12), 5341–5349 (2006).
[55]E. Bilkova, R. Pleskot, S. Rissanen, S. Sun, A. Czogalla, L. Cwiklik, T. Róg, I. Vattulainen, P. S. Cremer, P. Jungwirth, and Ü. Coskun, "Calcium directly regulates phosphatidylinositol 4,5-bisphosphate headgroup conformation and recognition," J. Am. Chem. Soc. **139**(11), 4019–4024 (2017).
[56]M. Javanainen, W. Hua, O. Tichacek, P. Delcroix, L. Cwiklik, and H. C. Allen, "Structural effects of cation binding to DPPC monolayers," Langmuir **36**(50), 15258–15269 (2020).
[57]J. L. R. Arrondo, F. M. Goñi, and J. M. Macarulla, "Infrared spectroscopy of phosphatidylcholines in aqueous suspension a study of the phosphate group vibrations," Biochim. Biophys. Acta, Lipids Lipid Metab. **794**(1), 165–168 (1984).
[58]S. Pullanchery, T. Yang, and P. S. Cremer, "Introduction of positive charges into zwitterionic phospholipid monolayers disrupts water structure whereas negative charges enhances it," J. Phys. Chem. B **122**(51), 12260–12270 (2018).
[59]H. Akutsu and Y. Kyogoku, "Infrared and Raman spectra of phosphatidylethanolamine and related compounds," Chem. Phys. Lipids **14**(2), 113–122 (1975).
[60]S. Roke, J. Schins, M. Müller, and M. Bonn, "Vibrational spectroscopic investigation of the phase diagram of a biomimetic lipid monolayer," Phys. Rev. Lett. **90**(12), 128101 (2003).
[61]R. Koynova and B. Tenchov, "Phase transitions and phase behavior of lipids," in *Encyclopedia of Biophysics*, edited by G. C. K. Roberts (Springer, Berlin, Heidelberg, 2013), pp. 1841–1854.
[62]H. Binder and K. Gawrisch, "Effect of unsaturated lipid chains on dimensions, molecular order and hydration of membranes," J. Phys. Chem. B **105**(49), 12378–12390 (2001).
[63]M. T. Hyvönen and P. T. Kovanen, "Molecular dynamics simulations of unsaturated lipid bilayers: Effects of varying the numbers of double bonds," Eur. Biophys. J. **34**(4), 294–305 (2005).
[64]F. Wei, W. Xiong, W. Li, W. Lu, H. C. Allen, and W. Zheng, "Assembly and relaxation behaviours of phosphatidylethanolamine monolayers investigated by polarization and frequency resolved SFG-VS," Phys. Chem. Chem. Phys. **17**(38), 25114–25122 (2015).
[65]N. Takeshita, M. Okuno, and T.-a. Ishibashi, "Molecular conformation of DPPC phospholipid Langmuir and Langmuir–Blodgett monolayers studied by heterodyne-detected vibrational sum frequency generation spectroscopy," Phys. Chem. Chem. Phys. **19**(3), 2060–2066 (2017).
[66]M. R. Watry, T. L. Tarbuck, and G. L. Richmond, "Vibrational sum-frequency studies of a series of phospholipid monolayers and the associated water structure at the vapor/water interface," J. Phys. Chem. B **107**(2), 512–518 (2003).